Egyptian Geophysical Society
EGS Journal, Vol. 13, No. 1, 1-12 (2015)

ANALYSIS OF SPECTRAL INVERSION APPROACH OF THE BOUGEUR GRAVITY DATA WITH AN APPLICATION TO ESH EL-MALLAHA AREA, SOUTHWESTERN GULF OF SUEZ, EGYPT

A. Gamal[(1)], A. Salem[(2)], K.S.I. Farag[(3)], A. Aref1 and S. Hamed[(3)]

(1) Airborne Geophysics Department, Exploration Division, Nuclear Materials Authority (NMA), Maadi 11728, Cairo, Egypt.
(2) Getech Group plc, University of Leeds, Kitson House،Elmete Hall،Elmete Lane، Leeds LS8 2LJ, England.
(3) Geophysics Department, Faculty of Science, Ain Shams University, Abbassia 11566, Cairo, Egypt.

دراسة تحليلية لتقنية عكسية فى النطاق الترددي للبيانات التثاقلية مع التطبيق على منطقة عش الملاحة - جنوب غرب خليج السويس- مصر

الخلاصة: تم تطوير العديد من النظم التثاقلية العكسية لكى تستخدم فى تحديد كل من التركيبات الجيولوجية التحتسطحية وأعماق الوصول الي الأحواض الرسوبية من البيانات التثاقلية المقاسة سواء فى النطاقات الترددية او الفضائية. لقد حاولنا فى هذه الدراسة تحليل و تقييم التقنية العكسية الخاصة بالعالم أولدنبرج حيث إن هذه التقنية تعتبر من أشهر التقنيات المستخدمة فى النطاق الترددى، وسوف يتم هذا التقييم بتطبيق دراستين إحداهما افتراضية و الأخرى حقيقية وخلال هذا التطبيق يتم استخدام نوع من التتابع الاستراتيجى العكسى الثلاثى الأبعاد. أولا النظرية العكسية و تحليل البيانات الافتراضية قد تم تطبيقها وهذه الدراسة الافتراضية الغرض منها تقييم مدى دقة و حساسية هذه التقنية العكسية الترددية للعالم أولدنبج لهذه النماذج البسيطة و المعقدة. اما عن تطبيق النظرية العكسية علي البيانات التثاقلية المقاسة فى منطقة عش الملاحة التى تعتبر من مناطق الحوضية الواعدة الحاملة للهيدروكربون فى منطقة خليج السويس المحدودة بطبقة القاعدة التصدعية المنكشفة على أعماق ضحلة و أيضاً على السطح ومن ثم هذا التطبيق الحقيقى الهدف منه هو اختبار تطبيقية هذه التقنية العكسية لكى تعطى أنسب نموذج كثافة طبقى يحاكى نتائج الآبار الحقيقية المحفورة فى منطقة الدراسة.

ABSTRACT: *Numerous inversion schemes have been developed to delineate both geological structures and depths of the sedimentary basin from the observed Bougeur gravity data either in spatial- or frequency-domain. In the present study we attempted to analyze and evaluate the 'Oldenburg's inversion approach', one of the most common spectral layered-earth inversion schemes, with applications to both synthetic and real data sets using a kind of sequential multi-dimensional inversion strategy. Inversion of the created synthetic data was first performed to determine how accurate and sensitive of such a spectral inversion approach would be for both simple and complicated geometric layered-density models. Inversion of the observed data at Esh El-Mallaha area, one of the most promising Southwestern Gulf-of-Suez hydrocarbon basins with faulted basement in Egypt, was then performed to examine the applicability of such a spectral inversion approach to obtain plausible layered-density models which can be correlated with the available stratigraphic-control well results.*

INTRODUCTION

In applied gravimetry, the Bougeur gravity data as a result of the earth are measured. This is what we might call a 'forward problem'; a model is given and the data are calculated. The forward (direct) problem is always uniquely solvable. It is often the other way around; data have been measured and we wish to derive a plausible layered-earth model that is consistent with the data, what may be described as 'inverse problem' which is concerned with the problem of making density interfaces (layer boundaries) from the measured data. Since nearly all field data are subjected to some uncertainty, these interfaces are statistically dependent, and therefore no inverse problem in gravimetric is uniquely solvable. Due to such an invariable non-linearity between the measured data and desired model parameters (layer densities and thicknesses), we usually use an iterative procedure in which the non-linear inverse problem is replaced, at each iteration, by its linearized approximation to be solved. Throughout, the data and model parameter vectors are related via a non-linear response function, which tells us how to calculate the synthetic data from the given model. The overall goal of the inversion is then to minimize the deviation between the measured and calculated data, what may be described as the 'objective function.' To derive an iterative inversion scheme, the response function is linearized about a starting model (initial guess) by expanding it into a Taylor's series approximation and ignoring the higher terms. This is the classical 'Gauss–Newton' solution (Marqardt, 1963; Lines and Treitel, 1984; Webring, 1985) which can be applied successively to improve (refine) the initial model until an optimal model update is obtained in an appropriate least-squares fashion. So, the process iterates until a given convergence criterion or a maximum number of iterations

is reached. To determine how well the model fits the measured data, the usual weighted least-squares criterion (Chi2 or root mean-square (RMS) misfit is used, attempting generally at minimizing the familiar estimate.

An unconstrained least-squares inversion like 'Gauss–Newton' approach has a difficulty when the gravimetric inverse problem is ill-posed and ill-conditioned, and hence the naive least-squares solution is completely dominated by contributions from data errors and rounding (perturbation) errors. Therefore, such a solution becomes inherently non-unique and even unstable. That means, one can find several very different layered-earth models fitting the measured data with approximately the same accuracy, but they are statistically unreliable. So, it is common to pose the problem as a non-linear optimization problem in which the penalized objective function Φ(m) comprises a residual norm, i.e., a measure of data misfit, Φd(m) and a regularized solution norm, i.e., a measure of discretized model character, Φm(m). For instance, by requiring the solution to minimize certain functionals in addition to the standard least-squares data fitting. This approach is known as the classical 'Tikhonov's regularization' (Tikhnov and Arsenin, 1977) Φ(m) =Φd (m) +λΦm (m).

Practically, regularization is necessary when computing a stable solution to gravimetric inverse problem. By adding regularization we are able to damp the error contributions and keep the regularized solution of reasonable size. This philosophy underlies the most regularization methods. However, all regularization methods for computing stable solutions to inverse problems involve a trade-off (regularization parameter) λ between the two terms of the objective function. What distinguishes the various regularization methods is how they measure these quantities, and how decide on the optimal trade-off between the two terms.

Layered-earth inversion of Bougeur gravity data can be carried out either in spatial- or frequency-domain. Spatial-domain techniques (Bott, 1960; Danes, 1960; Corbató, 1965; Tanner, 1967; Barbosa et. al., 1999) are inherently more flexible than frequency-domain techniques and more easily utilized for inversion schemes, as they separately calculate and totally sum the gravitational fields by breaking up the earth model into a set of simple-geometric subsurface objects in juxtaposed vertical fashion. On the other hand, frequency-domain inversion, using sum of fast Fourier transforms (FFT) of the gravitational anomaly (IEEE, 1967; Parker, 1973; Oldenburg, 1974; Pilkington and Crossley, 1986), is computationally time-consuming, than the spatial-domain techniques, particularly when the earth model is large, uneven or non-uniform, and when large quantities of data are available. But such a spectral inversion rapidly represents the anomaly data as the summation of cosine and sine series over a finite sequence of discrete uniformly spaced wavelengths which are fixed by the number of gridded data, and therefore the associated computations are more efficient, accurate and with a minimal number of assumptions.

A–Prior Information and Geologic Setting:

The Gulf-of-Suez is a Neogene regional extensional continental rift system that developed by the separation of the African and Arabian plates in Late Oligocene–Early Miocene, comprising a NW-trending marine basin of about 325 km long, with a maximum width of about 90 km at the northern terminus of the Red Sea (Fichera et al. 1992; Bosworth and McClay, 2001). The structural evolution of such a rift began by low-angle listric normal faulting and dyke injection, resulted in easterly-titled fault blocks in the form of half grabens (Said, 1962 and Meshref, 1990). By Middle to Late Miocene, an active subsidence, due to a probable crustal thinning, resulted in eastward movement of the rift axis toward the irregular axial grabens. Esh El-Mallaha structural block is part of the southern Gulf-of-Suez intra rift system that was subsequently deformed and uplifted in the Pliocene to Pleistocene/Holocene (Winn et al., 2001).

Esh El-Mallaha area is situated about 27 km southeast from Ras Shukir and about 75 km northwest from Hurghada along the southwestern coastal strip of Gulf-of-Suez. It is roughly centred at latitude 27° 53' N and longitude 33° 24' E (Figure 1), and easily accessible through the Ras Gharib–Hurghada highway. Both Gebels El Zeit (19 km long) and Esh El-Mallaha (65 Km long) basement complex elongated ranges represent the natural eastern and western shoulders of the study area, respectively, and composed mainly of Precambrian metamorphic and granitic rocks, and Dokhan volcanics (andesitic at Gebel El Zeit to rhyolitic at Gebel Esh El-Mallaha) (Said et al., 1994). These ranges are bounded and dissected by two main normal faults 'F1 and F2', trending in the NW–SE direction and lying parallel to the Gulf-of-Suez, that have juxtaposed outcrops against the sedimentary rocks (Figure 1) which are naturally exposed on the surface in several wadi sand filled with Quaternary alluvium (Farouk, 1965; Moustafa and Fouda, 1988). Such tectonic faults form a half-graben like structure and geologically enclosed a thick sedimentary succession at the central low lands of Pre-Cretaceous to Recent age and known as Gemsa–El Zeit Bay Basin (Angelier, 1985; Allam, 1988; Ismail, 1996 and 2012). The topographic relief of the study area is almost uneven, ranged between 2.5 (central lowlands) to 450.0 m (shoulder highlands) above sea level (Figure 2).

The deep structural pattern at the Gemsa–El Zeit Bay Basin is not well-documented due to the rare of drilled stratigraphic-control wells within the basin and the inadequate quality of two- and three-dimensional seismic reflection images beneath the thick Middle/Upper Miocene evaporite sequences (Taha et al., 2002).Therefore, conducting a deep-investigative potential-field survey, like gravimetry, can help improve the resolution of the subsurface earth model.

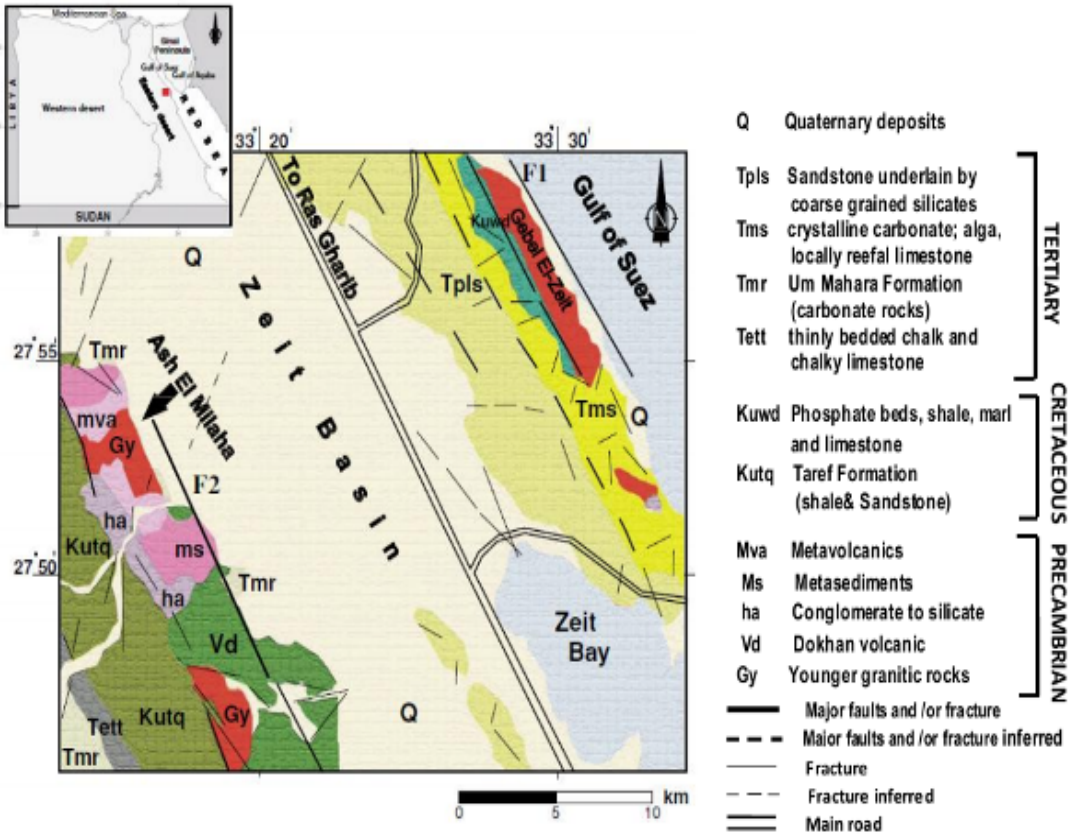

Figure (1): Location and regional geologic maps of Esh El-Mallaha area, Southwestern Gulf-of-Suez, Egypt (Modified after Conoco, 1987).

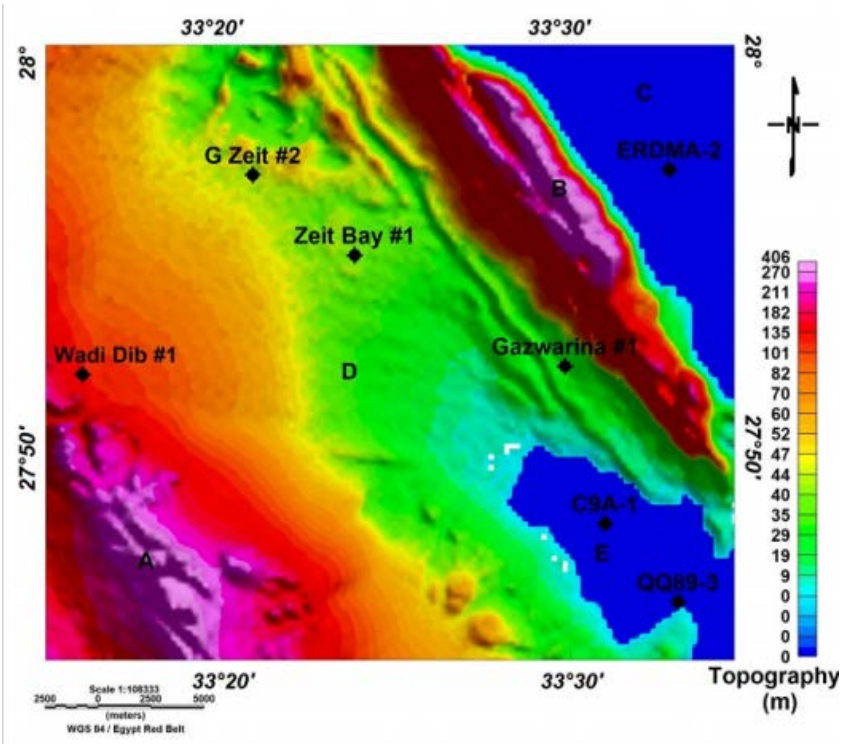

Figure (2): Regional topographic relief map of Esh El-Mallaha area, Southwestern Gulf-of-Suez, Egypt.

The available drilled stratigraphic-control wells at Esh El-Mallaha area which can be used as a-prior information both to built in the earth model throughout the inversion trials of the synthetic (forwardly calculated) data sets and to constrain the earth model throughout the inversion of the real data sets, and hence to improve the accuracy of the whole inversion process, are tabulated in table (1).

Table (1): The available drilled stratigraphic-control wells at Esh El-Mallaha area, south western Gulf-of-Suez, Egypt. These wells have been used by recent studies 'Aboud et al, 2005 & Abd El Naby et al, 2010.

Stratigraphic-control well	Well Name	Total Drilled Depth (m)	Reached Rock Unit
W1	Wadi Dib #1	3769	Basement Rocks
W2	G. Zeit #2	3743	Miocene
W3	Zeit Bay #1	4452	Upper Cretaceous
W4	Gazwarina # 1	2162	Basement rocks
W5	ERDMA–2	4051	Basement Rocks
W6	QQ89–3	2908	Basement Rocks
W7	C9A–1	2727	Basement Rocks

Bougeur Gravity Data

Since 1964 several surveys covering a large area of Egypt specially the Gulf of Suez were conducted by Philips Petroleum, General petroleum Company of Egypt (GPC), AMOCO, and GeoFisica. The gravity data was collected using the Lacoste and Worden gravimeter (Scintrex Inc., USA) with an effective reading accuracy of 0.01 mGal. Within the ten years (1974-1984) a great project plan executed by General Petroleum Company of Egypt (GPC) under the uspice of the Egyptian academy of scientific research and technology was reviewed by Bureau Gravimetrique International (IBG) at Paris was aiming to implement a gravity map of Egypt by the establishment of national base net covering the whole country and complementation of all the previous surveys which had been done by foreign companies in addition to the GPC's own surveys using worden gravimeters either for retying these previous surveys together or surveys new un-surveyed areas. The survey pattern of the study area formed almost a rectangle of 32 x 28 km and was oriented in the NE–SW direction to meet the pre-defined main geological strike of the study area. Readings were routinely repeated to ensure almost consistent data sets. The raw data were recorded and corrected for the global gravity reference field and space-dependant effects, and then exported to x, y, z form and gridded using an interval of 1000 m. The Bougeur gravity data of the whole study area were later plotted in the form of a colored contoured map (Figure 3). This helps visualize, process and invert the observed data.

Generally, the obtained Bougeur gravity contours at the study area are simple in nature. Three long-wavelength, moderate amplitude, NW–SE striking anomalies; two elongated gravity highs have a wide gravity low in between. This can be geologically translated as the natural eastern and western shoulders of Gebel El Zeit and Esh El-Mallaha basement complex outcropped ranges and the thick Gemsa–El Zeit Bay sedimentary Basin in the center. The western gravity high is a doublet anomaly, while the other two gravities are well-separated from their background. This may suggest the presence of transfer local faults cutting Gebel Esh El-Mallaha perpendicularly.

Inversion Methodology:

The principle difficulty with the layered-earth inversion of Bougeur gravity data to delineate sedimentary basin geometry, i.e., basement relief swells, troughs, and corresponding faulting, folding and intra-sedimentary structures, is the inherent non-uniqueness of the solution. Such non-uniqueness can be constrained by two free parameters: the presumed sedimentary section–basement complex density contrast $\Delta\rho$ and the level at which the inverted basement topography is calculated z. Otherwise, the ambiguity in the gravity interpretation is arisen.

Spectral layered-earth inversion of Bougeur gravity data using Oldenburg's scheme (IEEE, 1967; Parker, 1973; Oldenburg, 1974; Pilkington and Crossley, 1986), based on parker's forward Green's function calculation (Parker, 1973), is one of the quantitative interpretation techniques that can reduce the non-uniqueness of the multi-dimensional earth model. This is because it sets $\Delta\rho$ parameter to be fixed, i.e., homogenous per density layer, to detect the effect of the second parameter z on the gravitational anomaly data. Because computations within the inversion scheme involve primarily the sum of the Fourier transforms of powers of the perturbing basement topography which can be computed very quickly, this technique can easily accommodate large numbers of model points without greatly decreasing the numerical stability or greatly increasing the computation. Additionally, the desired solution can be empirically assured by application of a low-pass filter both to improve its iterative convergence and to guarantee non-negative density distribution.

Throughout, the gravitational anomaly data can be inverted directly by minimizing a properly designed objective function of a minimally structured density model subject to fitting the observations. The objective function has the ability to incorporate all available a-prior information into the inversion from previous

geological and geophysical knowledge about the density contrast or from the interpreter's understanding about the geologic setting and its relation to density. The inverted density model not only fits the anomaly data reasonably, but also has a realistic likelihood of representing the earth geology.

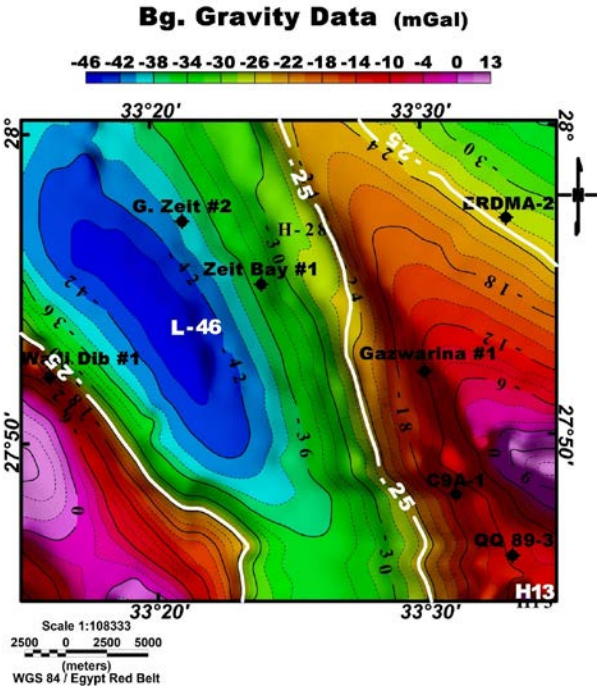

Figure (3): Observed Bougeur gravity contour map at Esh El-Mallaha area, Southwestern Gulf-of-Suez, Egypt. Contour interval is 2 mGal. Locations of the available drilled stratigraphic-control wells (W1 thru W7) are overlaid.

Inversion of Field Data:

Following any regularization method that concerns the idea of the minimally structured density model, we are seeking a reliable density model that represents a compromise between the residual norm (i.e. Chi2 data misfit) Φd(m) and the regularized solution norm (i.e. basement relief misfit) Φm(m) of the penalized objective function Φ(m). Therefore, if too much regularization is imposed on the regularized solution, then it will not fit the given data properly and the data misfit becomes large. On the other hand, if too little regularization is imposed then the fit will be good but the solution will be dominated by the contributions from the data errors, and hence the basement relief misfit will be too large. Having realized the important roles played by the norms of the regularized solution and residual, it is quite natural to plot these two quantities versus each other on double-logarithmic axes, i.e. as a curve parameterized by the regularization (or trade-off) parameter λ. This is usually referred as to 'L-curve' (Hansen, 1992). Practically, to find an appropriate choice for λ, the inversion is usually started several times with increasing λ stepwise throughout a wide range. In this case, if the Chi2 misfit is plotted against the basement relief misfit for that wide range of λ, the resulting curve tends to have a characteristic 'L-shape' (Figure 6, Upper). The corner, i.e., the point of maximum curvature, of this L-curve corresponds to a roughly equal balance of the two quantities (Hansen, 1999). Moving along the L-curve, away from the corner, is associated with a progressively smaller decrease in the data misfit for large increases in the basement relief misfit or with a progressively smaller decrease in the basement relief for large increases in the data misfit.

In the majority of the three-dimensional (3D) earth models inverted at the Esh El-Mallaha area, the L-curves do not always have a distinct corner at earlier iterations, whereas at later iterations they are developed well and, in this case, the L-curve criterion proves effective in determining the optimal λ. Figure 10 (Lower) shows 3D layered-earth inverted basement relief images at different λ thresholds below the study area. Here the data fit degrades significantly with increasing λ, while smaller λ results in rougher models. This clearly shows that the inversion results depend significantly on the value of the λ, an inappropriate choice for λ may create unwanted artificial features (artifacts) or even over-interpreted depth images. Occasionally, when λ is chosen too small, the solution shows oscillatory behaviour and even may become unstable, causing the data misfit to oscillate or even diverge, which means that no reliable model can be found (Schwalenberg et al., 2002).

The observed bougeur gravity anomaly data at Esh El-Mallaha area were extensively inverted in terms of 3D layered-earth density models using Oldenburg's spectral inversion scheme to accurately image the areal target basement relief. A detailed start density model fashion was first constructed based on a-prior information derived from the available drilled stratigraphic-control wells at Esh El-Mallaha area. The start basement topography, represented the arithmetic mean of the control well depths, taking into consideration the outcropped basement complex on both eastern and western shoulders, was initially introduced to the inversion. The presumed sedimentary section–basement complex density contrast Δρ for several inversion trials was gradually set between 0.10 and 1.0 g/cc and kept fixed laterally during the inversion run. Latter, the inverted basement relief images, corresponding to the used density contrasts, were consistently inspected.

Using GM–SYS inversion code, a constant regional offset or shift usually should be explicitly subtracted from the calculated gravity anomaly data to match the observed data, and hence to minimize RMS data misfit. This is necessary because the GM–SYS calculated data, by default, are absolute values for the layered-density model extending to 20,000 km in the both lateral directions and to 50 km deep.

Plotting the regularized solution norm, i.e.,

basement relief misfit, Φm(m) versus the used density contrasts Δρ at different regional offset thresholds, ranged between 0.0 to 12.0 mGal, on semi-logarithmic axes, (Figure 4) showed clearly that the effective starting density contrast is bounded between 0.30 and 0.40 g/cc.

For further optimization process aiming to bound more optimized model and data parameters; (Figure 5) involves four graphs explicate a tri-relationship between stabilizing filter , Convergence limit , and arithmetic mean depth Z_o , these graphs simplify the solution norm route mean square while using four convergence limit trials (i.e., 0.001, 0.01, 0.1, and 1 mGal) withal for each trial utilizing four cases of Z_o (i.e., -3,000, -3,500, -4,000, and -4,200 m) and applying nine filters L.H.C & U.H.C limits within the inversion run. Lastly, these graphs purpose to obtain an initial guess about the optimum of these three parameters together (Flt., Cnv. Limit, and Z_o) and also verify how? optimum the starting filter (3,000 - 4,000 m) which was haphazardly used thru the previous optimization process can be further treated as the final optimal one. As a result of this Figure 9 with its four graphs we conclude the verification of the starting filter to be optimum in existence of the mostly optimal Z_o set ranges in between -4,000 and -4,200 m and optimal set of convergence limit ranges in between 0.1 and 1 mGal.

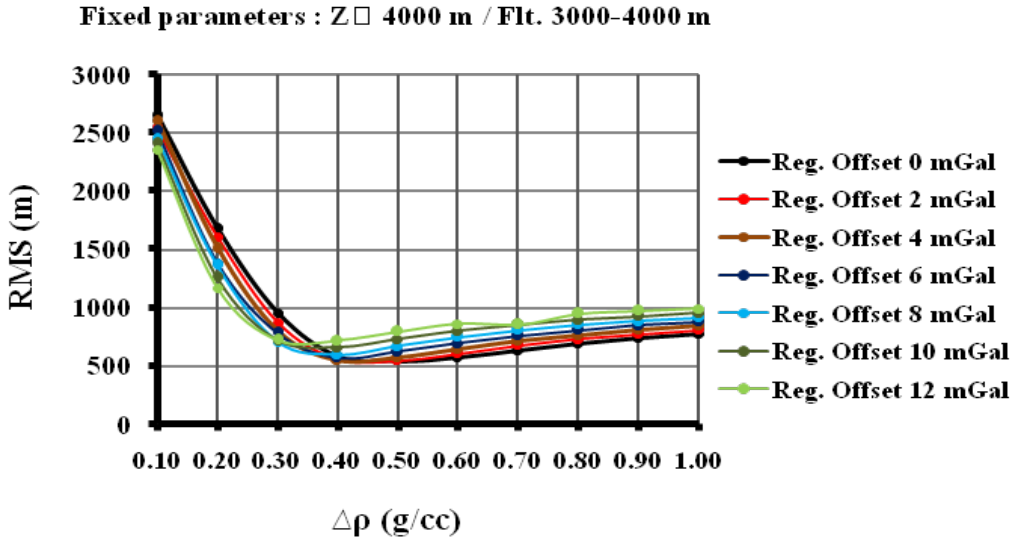

Figure (4): The obtained basement relief misfit RMS (m) versus the used density contrasts Δρ at different regional offset thresholds, ranged between 0.0 to 12.0 mGal.

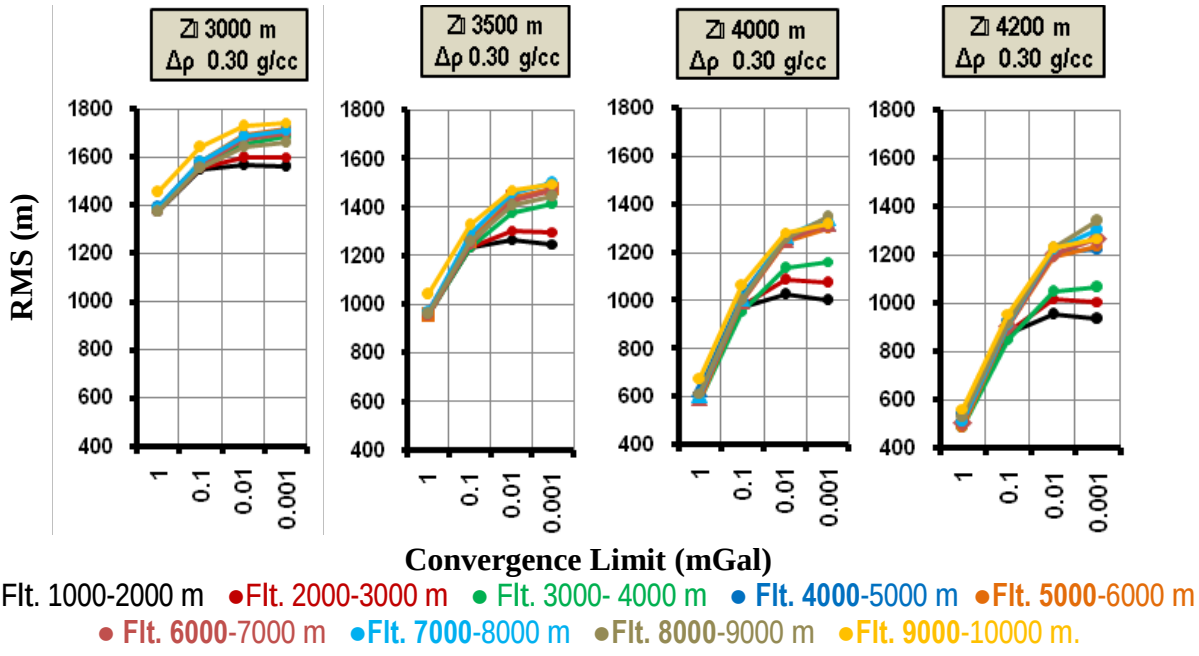

Figure (5): The obtained basement relief misfit Φm(m) versus the used convergence limit i.e., 0.001, 0.01, 0.1, and 1 mGal at four cases of different Z_o (m) i.e., 3000, 3500, 4000 and 4200 m & fixed Δρ 0.30 g/cc.

For detecting the optimum value of convergence limit to be utilized within the inversion run to inner constrain the difference in error standard deviation of the last two iterations to be lower than this convergence limit value; we plotted the L-curve to specify the optimum convergence limit at its nose so as to balance the relation between the solution misfit and data misfit,(Figure 6) illustrates this relationship and illuminates the optimum convergence limit equal 0.6 mGal, this value subset to the initial guess (i.e., in between 0.01 and 1 mGal) which was concluded from (Figure 5) so the specification of this convergence limit value verifies and proving true the optimization process. Behold! this L-curve was plotted for certain inversion run with these almost optimum parameters (i.e., Z_o - 4,200 m , Δρ 0.30 g/cc, and Flt. 3,000 - 4000 m) furthmore these random and non optimized parameters (i.e., Regional offset 0 mGal , cnv. limit 0.001 mGal , and Dc. Shift 25 mGal force mean error to be zero).

For further stabilizing and constraining the regularized solution, several gradual Density contrast Δρ trials between 0.10 to 1.00 g/cc with interval 0.10 g/cc were put to a test through the inversion process at the time of using the optimal filter 3000-4000 m and optimal convergence limit 0.6 mGal in addition fixed the starting arithmetic mean depth Z_o equal-4,200 m. Latter, the inverted basement relief images, corresponding to the operation of each Δρ trial, were consistently inspected and finally the optimal Δρ 0.37 g/cc were detected as its corresponding route mean square equal 441 m explicates the lowest value respecting the other trials (Figure 7 a, b).

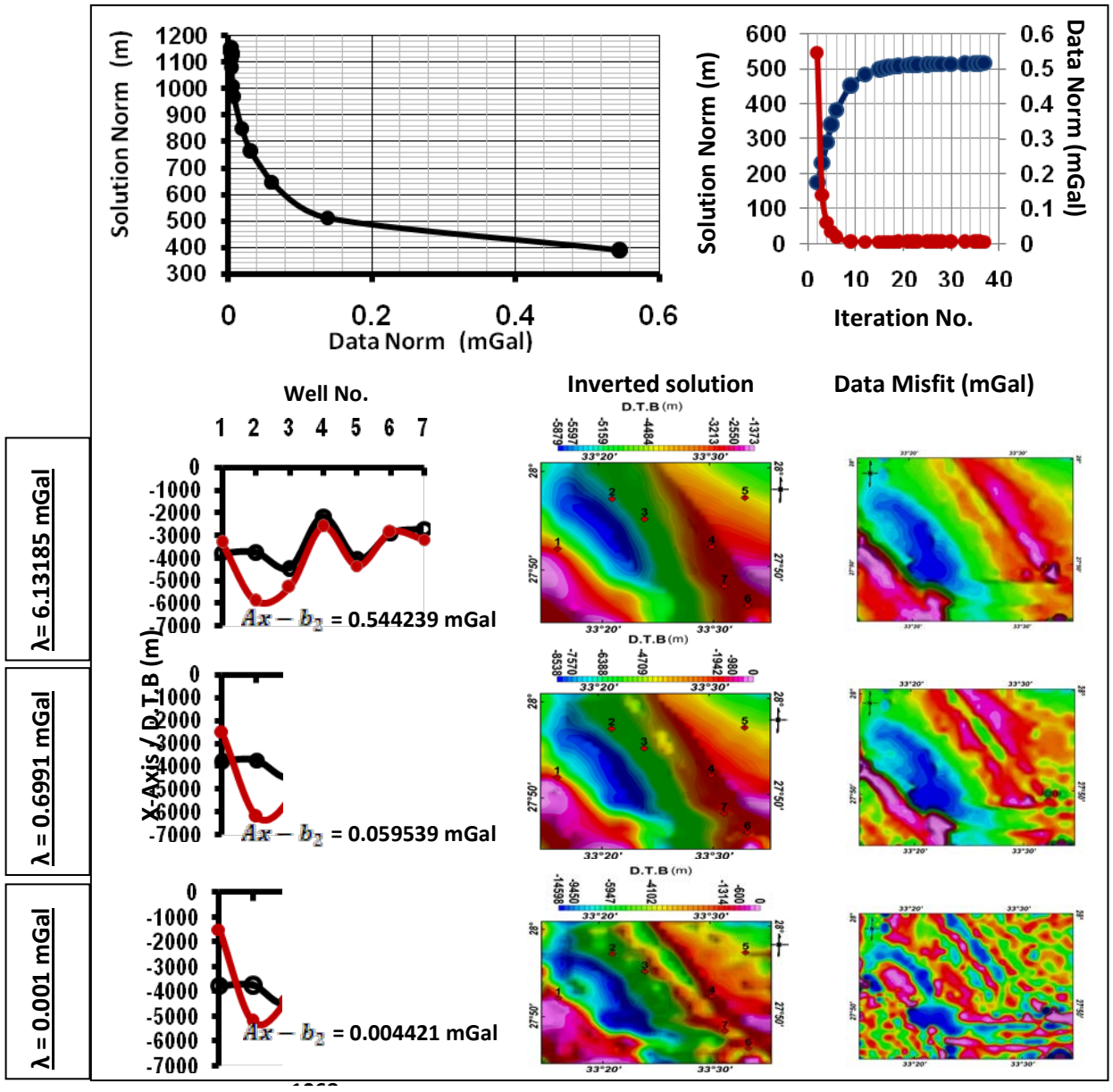

Figure (6): (Upper) The obtained L-curve, at different λ thresholds for several inversion runs, and the optimal λ for the 3D layered-earth inverted basement relief image below Esh El-Mallaha area. (Lower) Inverting using the optimal λ=0.699 represents an appropriate trade-off, while inverting using λ<0.699 and λ>0.699 represents under-conditioned (roughed) and over-conditioned (smoothed) density models, respectively.

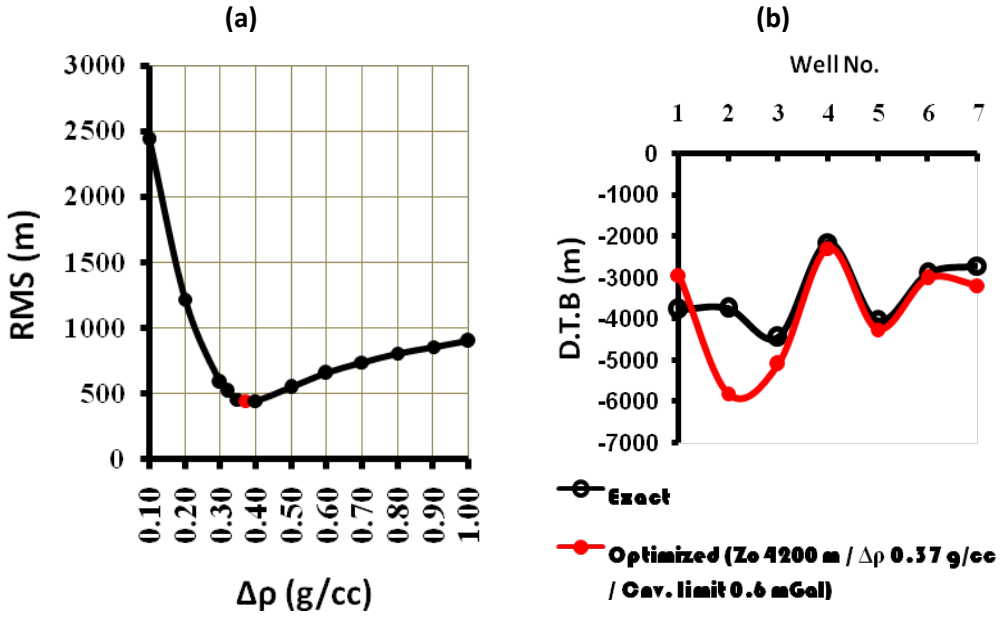

Figure (7 a, b): Optimization procedure for selecting the final optimum density contrast which probably matching the existent one of the study area.

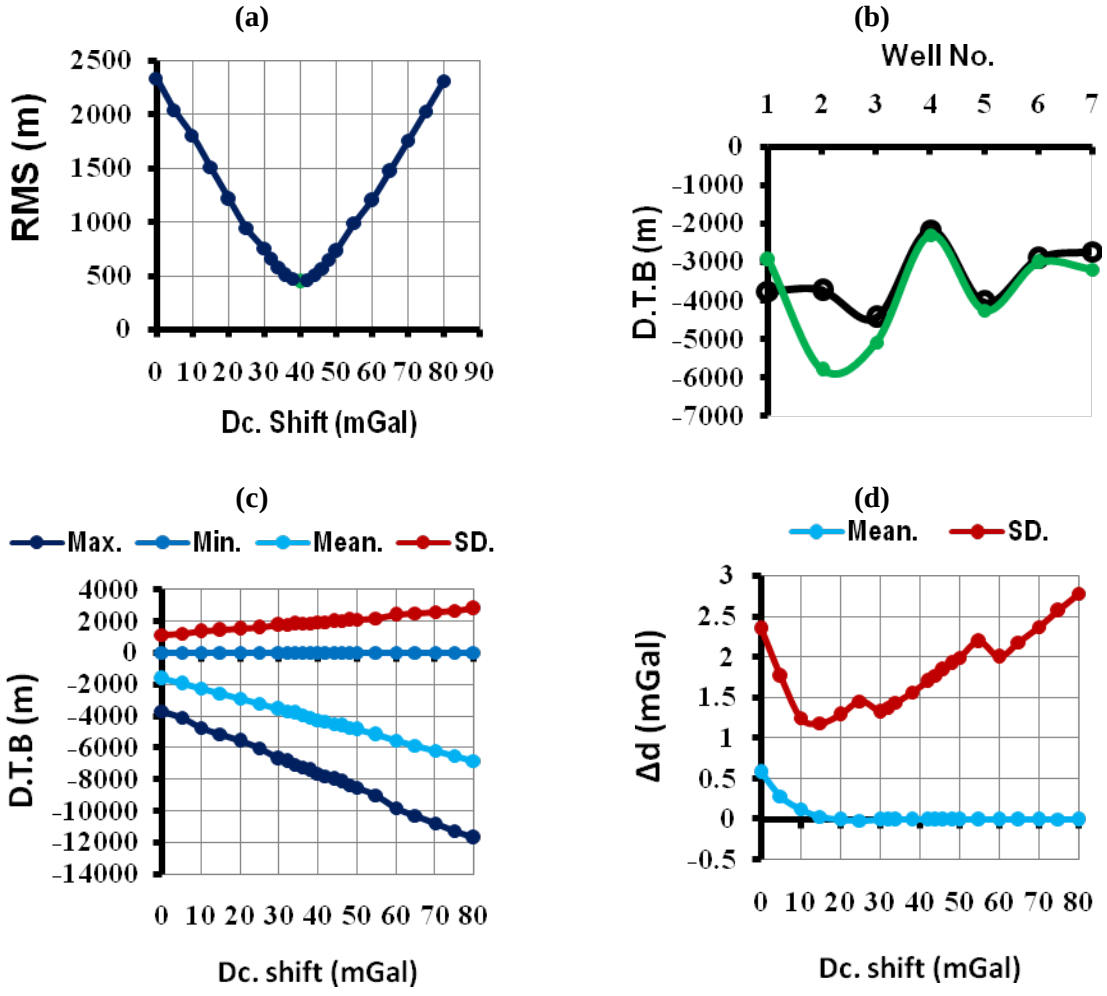

Figure (8 a, b, c, d): Optimization strategy for detecting the optimal Dc shift used to inner constrains the inversion run.

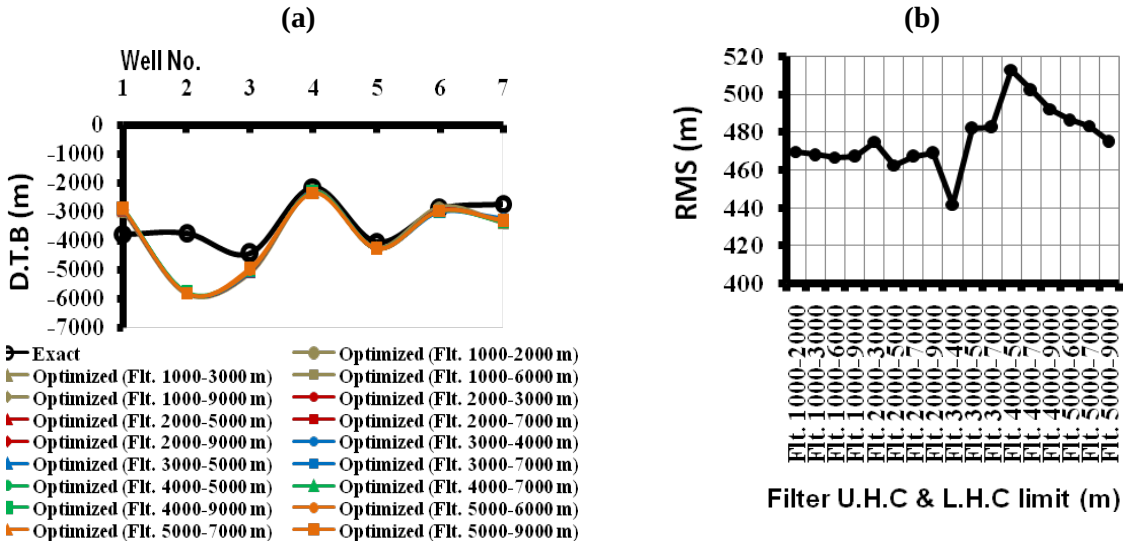

Figure (9 a, b): Stability procedure for detecting the optimum lower and upper high cut limits of the used filter for further obtaining the final stable solution.

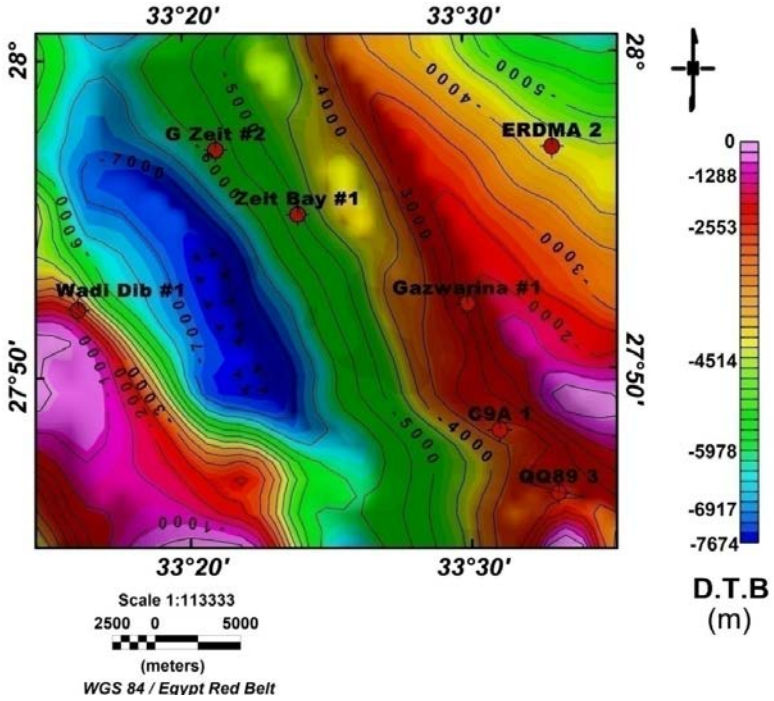

Figure (10): Optimal Inverted basement relief depth image of Esh El Mallaha field Bougeur gravity data. Contour interval is 500 m. Locations of the available drilled stratigraphic-control wells (W1 thru W7) are overlaid.

Finally to define the optimal Dc shift value which can be added to each iteration trial within the inversion run to inner constrain the results; We used several Dc shift trials ranged between 0 and 80 mGal. Latter, the optimal Dc shift value equal 40 mGal was defined and its corresponding route mean square illustrates the lowest value equal 441 m confirming the result of the previous process (Figure 7a). The inverted basement solution resulted from this constraint process with this route mean square value is expected to be the nearly optimal one (Figure 8 a, b & Figure 10).

Concerning this optimal solution (Figure 10) and despite the almost optimum it is, the resulted mean data misfit between its calculated response and the observed data (i.e., inverted data) nearly equal zero to resemble the zero regional offset subtracted constraint value which used within the inversion run (Figure 8 d) , this problem of generating an optimal solution with approximately zero mean of data misfit isn't preferred in gravity inverse modelling at which the sedimentary section has its considerable actual residual gravity effect and according to this resulted zero mean of the data misfit which represent the residual data the sedimentary section effect being neglected.

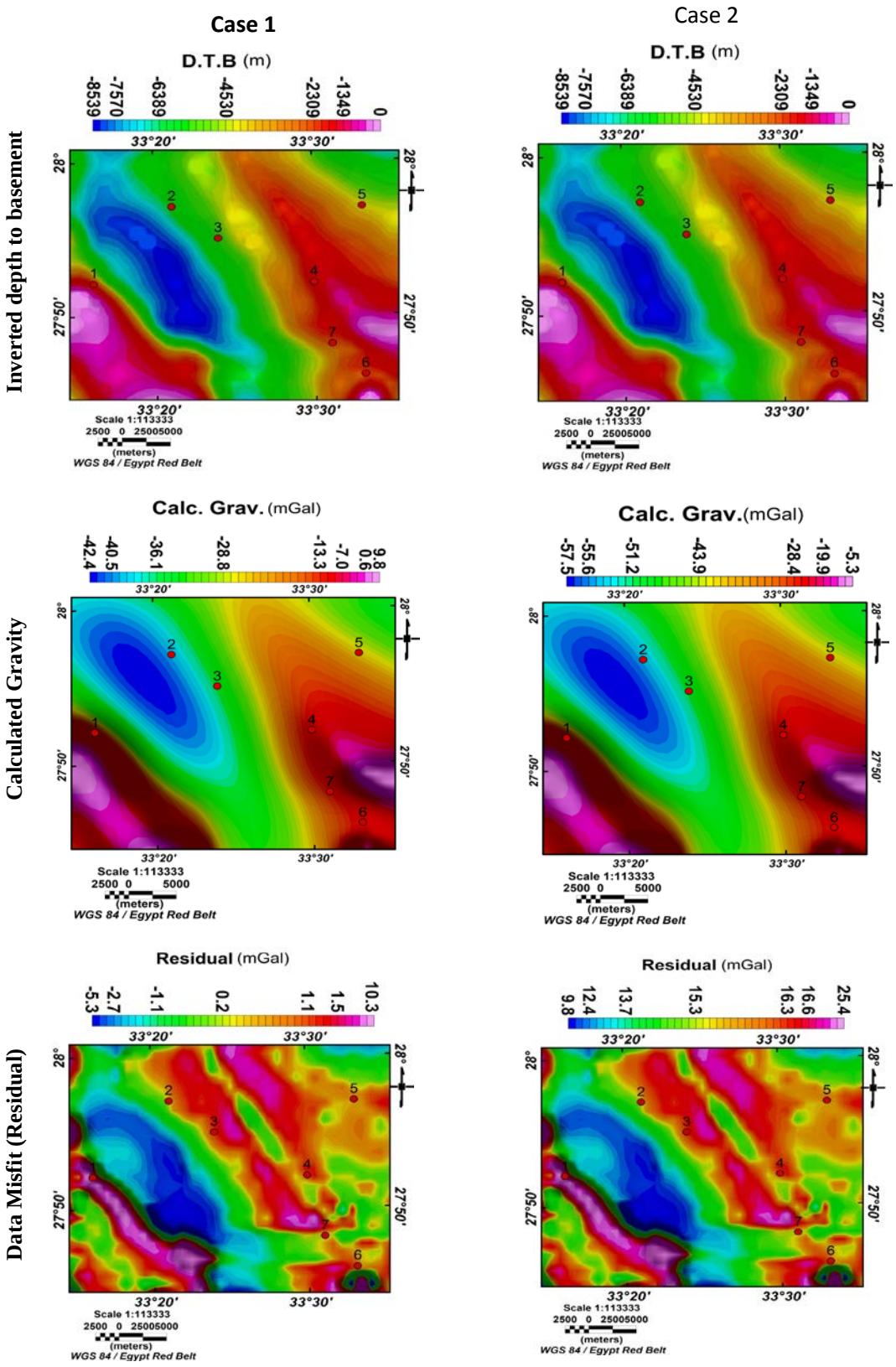

Inversion parameters: Flt 3000-4000/ Convergence limit 0.6 mGal/Δρ 0.30 g/cc/ $Z_0$4200 m/ Regional offset 0 mGal

Inversion parameters: Flt 3000-4000/ Convergence limit 0.6 mGal/Δρ 0.30 g/cc/ $Z_0$3000 m/ Regional offset 15.1 mGal

Figure (11): Factual Two cases reveal the non-uniqueness problem of the inversion process.

Also by QC the optimum of the inverted basement relief depth results according to minimum, maximum and mean depth respectively (Figure 8 c), there represent an acceptable results correlated with the prior information assumptions. (i.e., minimum depth = 0 m correlate with the prior information of basement out-cropping, maximum & mean depth (-7,674 & -4,253 m) respectively close to correlate the prior information assumption of maximum depth probably exists at set (-5,000 to -7,000) m & mean depth at set (-3,000 to -5,000) m. these prior information assumptions are summarized from previous aeromagnetic geophysical interpretation study has done on the same area (Aboud et al., 2005) and used only as a guide line for Qc and evaluating how much accepted the results are. Further For more evaluation tests we QC the total depth (T.D) results at the available actual five basement constraint wells W (1,4,5,6,7), and two un-reached basement constraint wells W (2,3); (Figure 8 b) illustrates that the inverted basement T.D depth at W (2,3) achieves the desired Qc tests of [W (2,3) inv. TD. > W (2,3) actual TD.] & [W (2) Inv. TD. > W (3) Inv. TD.] and also illustrates the approximately fitting between the actual and inverted T.D at W (1,4,5,6,7) to achieve the desired QC test of W (1,4,5,6,7) Inv. TD. = or ≅ W (1,4,5,6,7) actual TD., this approximately fitting images a bit accepted logical misfit owing to the use of homogenous Δρ through the inversion run whither this run against the reality existence of heterogeneous lateral and vertical density within each sub-surface layer generating variant density contrasts around the layers' interfaces.

For confirming the stability and constraint process of the final regularized solution, several cut-off filters were applied to the optimal inversion results, using a final optimal model parameters of density contrast Δρ 0.37 g/cc and ZI -4,200 m besides a convergence limit 0.6 mGal, Dc. shift 27 mGal, and regional offset 0 mGal. Plotting a relation between Filter against its corresponding route mean square result confirm the previous optimization processes which used the starting filter 3000-4000 m (Figure 9).

Case 1&2 clarify actual example of the inversion process non-uniqueness problem at which the two cases are represented by two optimization strategies with different inversion model and data parameters. These strategies finally lead to the same result of inverted depth to basement image (D.T.B) and different sedimentary section residual gravity effect (Figure 11).

CONCLUSION

In this paper, the authors applied sequential analysis using Oldenburg's spectral inversion scheme, attempting to add a new insight on the sub-structural setting of Esh El-Mallaha area. The scheme was applied to real data for mapping depth to basement using 3D inversion of gravity data. The results were nearly correlated with the constraints and prior information assumptions from the geological background of the area. Also its qualitative interpretation indicated the existence of useful and deep basin for oil accumulations. The basement relief image represents graben sub-structural system bounded by two major faults extended from ground surface to large depths. This relief has a mean depth approximately equal -4,250 m. the average density contrast between sedimentary and basement section nearly equals 0.37 g/cc, i.e. average density for sedimentary and basement are equal to 2.30 , 2.67 g/cc respectively.

While Oldenburg approach adding insight to the regional tectonics and subsurface features, this technique is sensitive to homogenous constant density layers. It would be much more problematic and restricted using in areas which are characterized by complex sub-structural setting with laterally and vertically distribution of density contrasts. Therefore with gravity inversion, careful selection and application of available control data is essential for the success of the process and more additional constraints together with depth estimation methods should be used to increase the confidence of basement mapping from gravity data. Furthermore, using few constraints may produce a biased solution non-optimized at some places of the study area. Moreover, it gives low information about the subsurface, extracted from large quantities of observed data.

Although Oldenburg approach tried to avoid the stability and uniqueness problems of the inversion process, these problems still exist as we can invert the observed data in terms of the basement relief depth image using many different optimization strategies with different model parameters produced equally optimized solutions nearly correlating the reality with different data misfit. So by this approach we cannot detect the exact data misfit which represents the residual data to be used for further stripping process of the sedimentary section formations. Concluding that this approach cannot treat the problem of the observed data interfering parameters as it cannot separate the effect of each parameter independently from the observed data.

It is recommended for more accurate results to be achieved, using variable lateral intervals of density contrasts and also incorporating a relation between the vertical density variation and the depth through the inversion process to simulate the reality as each of the sub-surface layers composed of random vertical and lateral distributed density variations. Also, we recommend incorporating constraint of gravity tensors for more detection of the basement boundaries in addition using mesh structure space domain inversion technique for more flexibility in obtaining detailed sub-structure density image.

REFERENCES

Andrson, H., Nash, C., 1997: Integrated lithostructural mapping of the Rossing area, Namibia using high resolution aeromagnetic, radiometric, Landsat data and aerial photographs, *Exploration Geophysics*, 28, 185-191.

Charbonneau, B.W., Holman, P.B., Hetu, R.J., 1997: Airborne gamma spectrometer magnetic-VLF survey of northeastern Alberta. *In* Exploring for minerals in Alberta: Geological Survey of Canada Geoscience contributions, edited by MacQueen, Canada-Alberta agreement on mineral development. Geological Survey of Canada Bulletin 500, 107-132.

Conoco Inc., 1987: Stratigraphic lexicon and explanatory notes to the geological map of Egypt 1:500,000. Conoco Inc., Cairo, Egypt, 1989, 262p.

Cook, S.E., Corner, R.J., Groves, P.R., Grealish, G.J., 1996: Use of airborne gamma radiometric data for soil mapping. *Aust. J. Soil Res.*, 34, 183-194.

Darnley, A. G., and Ford, K. L., 1989, Regional airborne gamma-ray syrvey: A review; in "Proceedings of Exploration 87: Third Decennial International Conference on Geophysical and Geochemical Exploration for Minerals and Ground Water", Geol. Surv. of Canada, Special Vol. 3, 960 p.

Duval, J.S., 1983: Composite color images of aerial gamma-ray spectrometric data, *Geophysics*, 48, 722-735.

Ford, K.L., Savard, M., Dessau, J.-C. and Pellerin, E., 2001: The role of gamma-ray spectrometry in radon risk evaluation: A case history from Oka, *Quebec. Geoscience Canada*, 28, 2.

Graham, D.F., Bonham-carter, G.F., 1993: Airborne radiometric data: a tool for reconnaissance geological mapping using a GIS, *Photogrammetric Engineering and Remote Sensing*, 58, 1243-1249.

Grasty, R.L., Shives, R.B.K., 1997: Applications of gamma ray spectrometry to mineral exploration and geological mapping, Workshop presented at Exploration 97: Fourth Decennial Conference on Mineral Exploration.

Jaques, A.L., Wellman, P., Whitaker, A., Wyborn, D., 1997: High resolution geophysics in modern geological mapping. *AGSO Journal of Australian Geology & Geophysics*, 17, 159-174.

Lahti, M., Jonsen, D.G., Multala, J., Rainey, M.P., 2001: Environmental applications of airborne radiometric surveys. Expanded Abstracts, 63rd Annual Conference, European Association of Geoscientists and Engineers.

Lo, B.H., Pitcher, D.H., 1996: A case history on the use of regional aeromagnetic and radiometric data sets for lode gold exploration in Ghana. Annual Meeting Expanded Abstracts, Society of Exploration Geophysicists, 592-595.

Minty, B.R.S., 1997: Fundamentals of airborne gamma ray spectrometry. AGSO Journal of Australian Geology and Geophysics, v. 17, n. 2, 39-50.

Sanderson, D.C.W., Allyson, J.D., Tyler, A.N., Scott, E.M., 1995: "Environmental applications of airborne gamma ray spectrometry," Application of Uranium Exploration Data and Techniques in Environmental Studies, IAEA-TECDOC-827, IAEA, Vienna, 71-79.

Wilford, J.R., Bierwirth, P.N., Craig, M.A., 1997: Application of airborne gamma-ray spectrometry in soil/regolith mapping and applied geomorphology, *AGSO Journal of Australian Geology and Geophysics*, 17, 201-216.